

# Research and Analysis on the Durability of the Chassis of the Shallot Planting Machine

**Hau Le Trung**

Vinh Long University of Technology Education, Vietnam  
hault@vlute.edu.vn (corresponding author)

**Phi Cao Hung**

Vinh Long University of Technology Education, Vietnam  
caohungphi@vlute.edu.vn

**Quang Nguyen Thanh**

Hanoi University of Industry, Vietnam  
quangamk@gmail.com

**Dang Nguyen Thuan Hai**

Vinh Long University of Technology Education, Vietnam  
dangnth@vlute.edu.vn

*Received: 22 October 2025 | Revised: 15 November 2025 and 4 December 2025 | Accepted: 9 December 2025*

*Licensed under a CC-BY 4.0 license | Copyright (c) by the authors | DOI: <https://doi.org/10.48084/etasr.15705>*

## ABSTRACT

A combination of Finite Element Analysis (FEA) and frequency response simulation is utilized to evaluate the structural durability of a shallot planting machine operating on uneven pavement through. The evaluation was performed by developing a detailed three-dimensional model, comprising 15,322,319 nodes and 8,794,097 elements. Furthermore, excitation forces from the pavement were modeled within a frequency range of 0–150 Hz, revealing a resonance peak at 128 Hz. At this frequency, the maximum stress reached 275 MPa and the maximum deformation was observed at 7.6438 mm, exceeding the safety threshold. In addition, optimization techniques, including parametric adjustments and topology optimization, led to the reduction of structural mass by 15%, deformation by 25%, maximum stress by 20%, and the increase of stiffness by 10%. Consequently, the safety factor improved from 1.29 to 1.61. In addition, a dynamic model was developed in MATLAB to validate the FEA results, with a discrepancy of less than 5%. The findings provide a robust scientific foundation for enhancing the mechanical strength, vibration resistance, and service life of agricultural machinery under dynamic loading conditions.

*Keywords-shallot planter; structural durability; vibration analysis; topology optimization; finite element analysis*

## I. INTRODUCTION

Agricultural mechanization enhances the efficiency of agricultural production, particularly for specialized crops such as shallots. Shallot planters reduce labor, time, and costs while improving crop productivity and quality [1]. However, the design and durability of these machines are affected by uneven or bumpy surfaces, where dynamic excitation forces act with variable amplitudes and frequencies. These forces induce vibrations leading to dynamic stress on the machine's chassis. As a result, localized deformations develop, progressively leading to material fatigue, and ultimately structural failure. Additionally, excessive vibrations compromise planting accuracy affecting crop yield and quality.

In [2], a detailed model of the shallot planter was developed to assess stress and deformation within the frequency range of 0–150 Hz. The analysis focused on the identification of resonance frequencies and proposed improvements to mitigate relevant risks. The durability and stability of the chassis are critical to the performance and longevity of agricultural machinery, as they must withstand dynamic loads, vibrations, and harsh environmental conditions [3-5]. Authors in [6] demonstrated that suboptimal chassis designs lead to excessive vibrations, reduced planting precision, and premature equipment failure. Methods, such as Computer-Aided Design (CAD) and FEA, have been employed to evaluate stress distribution, deformation, and potential failure points under real-world operating conditions [7]. These types of simulations

facilitate chassis optimization, enhance durability, reduce material usage, and extend equipment lifespan [8, 9].

The shallot planter system analyzed in this study consists of a specialized planting mechanism driven by a Kubota L4508VN tractor. The tractor transmits motion through an articulation system, propelling the planter according to a designed transmission ratio [1]. Uneven load distribution or inappropriate travel speeds can exacerbate vibrations, significantly impacting the system's performance [10]. Authors in [11, 12] investigated vibration characteristics through time and frequency domain analyses to assess interactions between components, identify primary vibration sources, and propose design improvements to minimize vibrations during operation. Moreover, the resonance and vibration phenomena of the chassis were analyzed to determine natural frequencies and mode shapes, enabling structural enhancements to improve operational performance [13]. Authors in [14] analyzed the vibration characteristics at the operator's seat position on a shallot harvester, identifying the influence of mechanical vibration on operator's comfort and machine stability.

However, most existing studies have focused on commonly used agricultural machinery such as seeders, seedling transplanters, and harvesters. There has been no comprehensive investigation into the vibration modeling of shallot planter assemblies. Particularly, no study has focused on the actual field conditions of the Mekong Delta, where cultivation practices and soil characteristics are highly distinctive. The current study aims to address this research gap.

The findings of this study are not limited to shallot planters but can be applied to any agricultural machinery operating under similar conditions. The analytical methods and computational tools developed provide a foundation for optimizing design, enhancing reliability, and extending the service life of various agricultural equipment, thereby contributing to sustainable agricultural mechanization.

## II. MATERIALS AND METHODS

### A. Scientific Basis of Research

This study evaluates the structural durability of a shallot planter under vibrations induced by uneven terrain. It integrates mechanical vibration theory, FEA, and frequency response analysis.

#### 1) Dynamic Equilibrium Equation

The dynamic equilibrium equation for a multi-degree-of-freedom system in FEA is expressed by:

$$[M]\{\ddot{u}\} + [C]\{\dot{u}\} + [K]\{u\} = \{F(t)\} \quad (1)$$

where  $[M]$ ,  $[C]$ , and  $[K]$  represent the mass, damping, and stiffness matrices, respectively,  $u$  is the nodal displacement vector, and  $F(t)$  is the time-dependent external force vector.

#### 2) Frequency Response Equation

Frequency response analysis determines the oscillation amplitude at each excitation frequency, enabling the calculation of stresses and strains. In the frequency domain, the dynamic equilibrium equation is reformulated as:

$$(-\omega^2[M] + i\omega[C] + [K])\{u(\omega)\} = \{F(\omega)\} \quad (2)$$

Furthermore, the displacement vector in the frequency domain is determined by:

$$\{u(\omega)\} = [H(\omega)]\{F(\omega)\} \quad (3)$$

where  $[H(\omega)]$  is the transmission function matrix and is calculated through:

$$[H(\omega)] = (-\omega^2[M] + i\omega[C] + [K])^{-1} \quad (4)$$

### 3) Application of FEA in Shallot Planter Vibration Analysis

For the vibration analysis of the shallot planter of this study, an FEA model was utilized comprising 15,322,319 nodes and 8,794,097 elements. This model simulated structural behavior under dynamic loading conditions. By applying appropriate boundaries and load conditions, the model determined the natural frequencies and corresponding mode shapes, the stress and strain distributions at each excitation frequency, and the locations of high stress concentration. This detailed model enables accurate prediction of the structural response to dynamic excitations, facilitating the identification of critical areas prone to failure.

### 4) Methods for Optimizing Agricultural Machinery Structures

#### a) Structural Parameter Optimization

Structural parameter optimization aims to identify optimal values for design parameters such as dimensions, thickness, and material properties. Consequently, mass can be minimized and stiffness maximized while durability constraints are satisfied. The optimization problem is formulated by:

$$\begin{cases} \min f(x) \\ \text{subject to } g_i(x) \leq 0, i = 1, 2, \dots, m \\ h_j(x) = 0, j = 1, 2, \dots, p \end{cases} \quad (5)$$

where  $f(x)$  is the objective function,  $g_i(x)$  represents inequality constraints, and  $h_j(x)$  denotes equality constraints.

#### b) Shape and Topology Optimization

Topology optimization aims to determine the optimal material distribution within a defined design space to maximize stiffness while minimizing mass. This approach is particularly effective for complex structures, such as the chassis of a shallot planter. The topology optimization problem is expressed by:

$$\begin{cases} \min c(\rho) = \{F\}^T \{u\} \\ \text{subject to } V(\rho) \leq V_0 \\ \text{and } 0 \leq \rho_i \leq 1, i = 1, 2, \dots, n \end{cases} \quad (6)$$

where  $c(\rho)$  is the structural compliance,  $V(\rho)$  is the material volume,  $V_0$  is the allowable volume limit, and  $\rho_i$  is the density variable for the  $i$  element.

#### c) Optimization Algorithms and Tools

This study also employs the Solid Isotropic Material with Penalization (SIMP) algorithm, implemented within the ANSYS Workbench solver in the Mechanical APDL environment. The objective of optimization is to minimize structural mass while satisfying constraints on stress, strain, and resonance frequency. The optimization process consists of

three stages: defining the design space, applying constraints, and iterating until convergence of the optimization criteria.

To evaluate the optimization, two harmonic response analyses were conducted with identical input excitations but with varying structural parameters of the chassis beam. Specifically, the analyses compared configurations before and after optimization by varying the height to width ratio of the beam's cross-sectional profile. The FEA results for stress and deformation are illustrated in Figures 1 and 2, respectively, and in Table I.

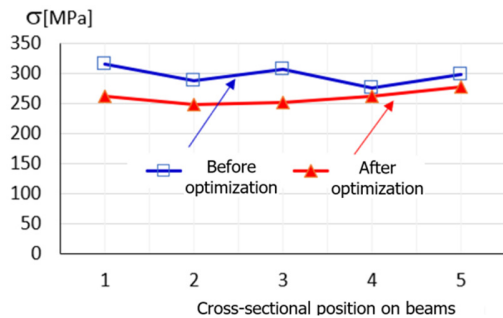


Fig. 1. Comparison of maximum stress values of configurations before and after optimization.

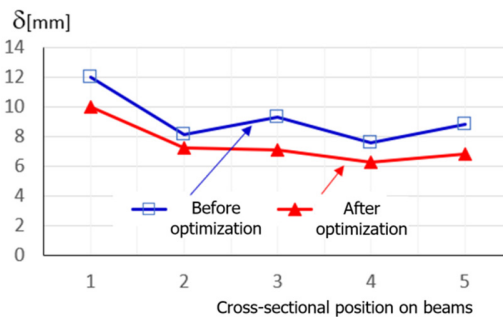


Fig. 2. Maximum deformation values of configurations before and after optimization.

TABLE I. MAXIMUM STRESS AND DEFORMATION VALUES BEFORE AND AFTER OPTIMIZATION

Before optimization	After optimization
<b>Stress (MPa)</b>	
315	261
288	248
306	252
275	261
298	277
<b>Deformation (mm)</b>	
12	10
8.1	7.2
9.3	7.1
7.6	6.3
8.8	6.8

### 5) Dynamic Model of Excitation from Uneven Terrain

#### a) Pavement Characteristic Model

The unevenness of pavement is characterized by using the Power Spectral Density (PSD) function, expressed by:

$$\Phi(n) = \Phi(n_0) \left(\frac{n}{n_0}\right)^{-\omega} \tag{7}$$

where  $\Phi(n)$  is the PSD of pavement unevenness,  $n$  is the spatial frequency,  $n_0$  is the reference spatial frequency,  $\omega$  is the waviness coefficient, and  $\Phi(n_0)$  is the PSD value at the reference frequency.

#### b) Conversion from Pavement Model to Excitation Force

The excitation force acting on the wheels of the shallot planter is derived from the pavement model through a transfer function relating surface unevenness to contact force, given by:

$$F(t) = k_{tire}[z_r(t) - z_s(t)] + c_{tire}[\dot{z}_r(t) - (\dot{z}_s(t))] \tag{8}$$

where  $F(t)$  is the contact force between the wheel and the pavement,  $k_{tire}$  is the tire stiffness,  $c_{tire}$  is the tire damping coefficient,  $\dot{z}_r(t)$  is the pavement surface height, and  $\dot{z}_s(t)$  is the vertical position of the wheel. The amplitude of the excitation force in the frequency domain depends on the pavement characteristics and the machine's travel speed. Figure 3 depicts the displacement amplitude of the chassis against the frequency.

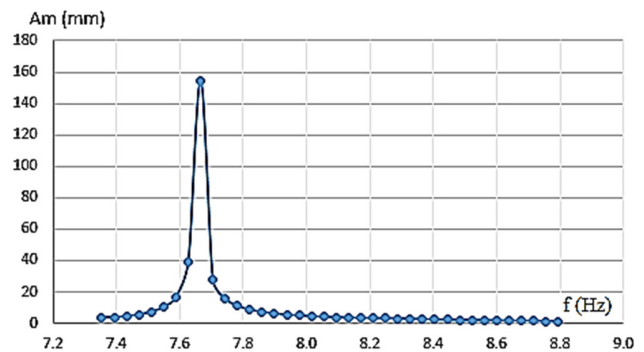


Fig. 3. Frequency amplitude of the excitation force from a unit pavement irregularity.

According to Figure 3, the displacement amplitude remains low at near zero excitation frequencies and increases sharply as the system approaches resonance. A peak, corresponding to the maximum amplitude value, is observed between 7.6 Hz and 7.7 Hz. Furthermore, near zero, values of amplitude are observed or frequency values higher than 7.8 Hz. In the frequency range of 0–15 Hz, the relative amplitude of the excitation force varies, as detailed in Table II.

TABLE II. RELATIVE AMPLITUDE OF THE EXCITATION

Frequency (Hz)	Amplitude effect
0–1	0.05
1–2	Increases from 0.05 to 0.2
2–4	Decreases from 0.2 to 0.05
4–7	Increases from 0.05 to 0.35
7–10	Increases from 0.35 to 0.5
10–13	Decreases from 0.5 to 0.3
13–15	Decreases from 0.3 to 0.1

This relative amplitude is converted to an actual excitation force by multiplying it by a standard force value.

6) Durability Theory of Agricultural Machinery Structures

The structural durability of the shallot planter is ensured when the maximum stress in the structure does not exceed the stress threshold, as defined by:

$$\sigma_{max} \leq [\sigma] = \frac{\sigma_y}{n} \tag{9}$$

where  $\sigma_{max}$  is the maximum stress,  $[\sigma]$  is the allowable stress,  $\sigma_y$  is the material yield strength, and  $n$  is the safety factor typically ranging from 1.5 to 2.5 for agricultural machinery. The endurance condition is expressed as:

$$\frac{\sigma_a}{\sigma_{-1}} + \frac{\sigma_m}{\sigma_y} \leq 1 \tag{10}$$

where  $\sigma_a$  is the stress amplitude,  $\sigma_m$  is the mean stress,  $\sigma_{-1}$  is the fatigue limit of the material, and  $\sigma_y$  is the yield strength.

III. MODELING AND SIMULATION

A. Modeling of the Shallot Planter

1) Mechanical Modeling

The shallot planter is modeled as a complex mechanical system comprising the following main components: the main frame, which supports the entire system; the planting mechanism, including the seed distribution box and planting structure; the transmission system, which consists of shafts, gears, and chains; and the wheels, which interact with the pavement surface.

During the dynamic analysis, the shallot planter is represented as a multi-mass, multi-degree-of-freedom system, interconnected by elastic and damping elements. Excitation loads are transmitted from the pavement through the wheels to the chassis, as depicted in Figure 4.

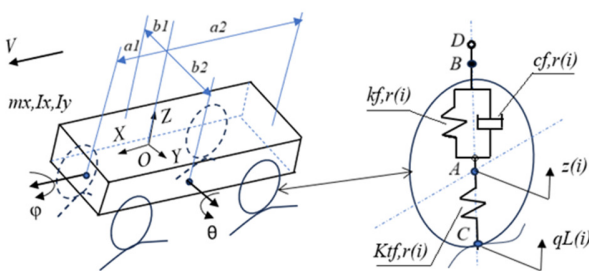


Fig. 4. Shallot planter model.

2) Finite Element Model

To ensure the accuracy and reliability of the FEA, a mesh convergence study was conducted to evaluate the sensitivity of the simulation results with respect to mesh density. Three mesh configurations were tested by varying the average element size: a coarse mesh of approximately 5.2 million elements, a medium mesh of approximately 8.8 million elements utilized in the main analysis, and a fine mesh of approximately 12.6 million elements. A detailed three-dimensional model,

illustrated in Figure 5, of the shallot planter was developed in ANSYS Workbench with the following specifications:

- Number of nodes: 15,322,319
- Number of elements: 8,794,097
- Element type: SOLID185 (8-node solid element)
- Material properties: Structural steel (E = 2,1×10<sup>5</sup> MPa, ν = 0,3, ρ = 7850 kg/m<sup>3</sup>)

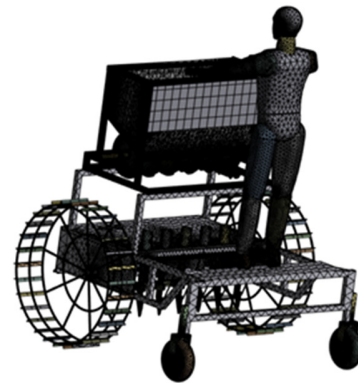


Fig. 5. Finite element model of shallot planting machine.

The mesh was refined with higher density at critical regions, such as corners, joints, and areas with abrupt geometric changes, to accurately capture stress concentrations. FEA was performed in ANSYS Workbench to evaluate stress and deformation distributions in the chassis.

B. Dynamics Simulation and Analysis

1) Free Vibration Analysis

A free vibration analysis was conducted to determine the natural frequencies and corresponding mode shapes of the shallot planter. The first natural frequency was observed at 14.2 Hz (vertical vibration mode), the second at 28.7 Hz (torsional vibration mode), the third at 63.5 Hz (horizontal bending mode), and the fourth at 128 Hz (longitudinal bending mode). The last one exhibits the largest amplitude in the central region of the chassis, where the planting mechanism is mounted.

2) Frequency Response Analysis

Frequency response analysis was performed over a frequency range of 0–150 Hz with a step size of 0.5 Hz. The model was subjected to the following boundary and loading conditions. As illustrated in Figure 6, displacement constraints were applied at the wheel attachment points. In addition, vertical excitation forces from the pavement were employed at the wheel contact points. The results indicated that in the low-frequency range (0–50 Hz) the structure exhibited moderate deformation and stress, ranging from 1–3 mm and 50–100 MPa, respectively. In the mid-frequency range (50–100 Hz), the deformation and stress increase gradually, reaching 3–5 mm and 100–200 MPa, respectively. Finally, in the resonance region (near 128 Hz), the deformation and stress peak, reaching maximum values of 7.6438 mm and 275 MPa, respectively.

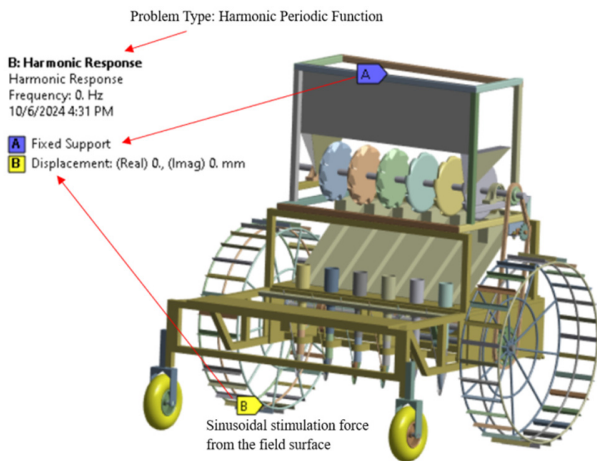


Fig. 6. Load setting model and edge conditions.

3) Detailed Analysis at Resonance Frequencies

At the resonance frequency of 128 Hz, the analysis revealed that the maximum deformation location appears at the central region of the chassis, where the planting mechanism is attached. Similarly, the maximum stress location is located at joints between the horizontal and longitudinal beams, particularly at corners and areas with cross-sectional changes. The dynamic gain factor was observed ten times the static response. Finally, the safety factor was calculated to be 1.29, below the proposed minimum threshold of 1.5 for agricultural machinery.

IV. RESULTS AND ANALYSIS

A. Stress and Deformation Spectrum Analysis

The stress and deformation spectra were plotted as functions of frequency, as presented in Figures 7 and 8. The spectra indicate that the deformation increases with frequency, peaking at 128 Hz before decreasing. Stress closely correlates with deformation, also peaking at 128 Hz, while the stress spectrum mirrors the deformation spectrum but with different amplitudes. Additionally, the spectra exhibit distinct peaks at the system's natural frequencies.

The deformation color map displayed in Figure 7 indicates that the region of maximum deformation is concentrated in the central chassis, while areas near the wheel attachment points exhibit minimal deformation. Furthermore, in the normal operating frequency range (<50 Hz), deformation remains within acceptable limits. At 128 Hz, the maximum deformation on the chassis is 7.6438 mm. Figure 8 presents the stress distribution, with a maximum stress of 275 MPa on the chassis at the resonance frequency of 128 Hz. At the resonance frequency, stress exceeds the allowable limit. Other frequency ranges exhibit stresses below the threshold.

There are four main improvements that can be made to the structure. To begin with the structural design, high stress concentration regions must be reinforced, while ribs and joists should be placed at locations exhibiting significant deformation. This modification will increase chassis stiffness to shift the natural frequency away from the operating frequency range. Moreover, higher-strength steel should be used for

components subjected to higher stress. Vibration-absorbing materials at pavement contact points should also be incorporated. Furthermore, additional damping elements can be introduced to increase the damping ratio from 0.05 to 0.1–0.15. A suspension system to reduce the amplitude of vibrations transmitted to the chassis should also be implemented. Finally, operating speeds must be limited to avoid excitation frequencies near 128 Hz. The operating frequency range below 90 Hz was proposed to ensure a safety factor greater than 1.5.

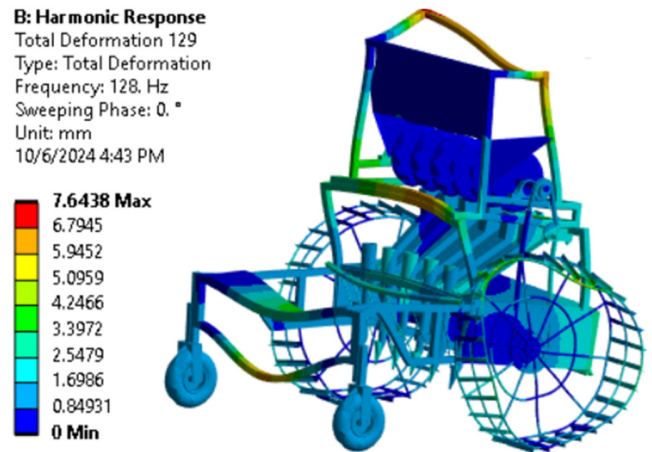


Fig. 7. Deformation distribution results on the working machine.

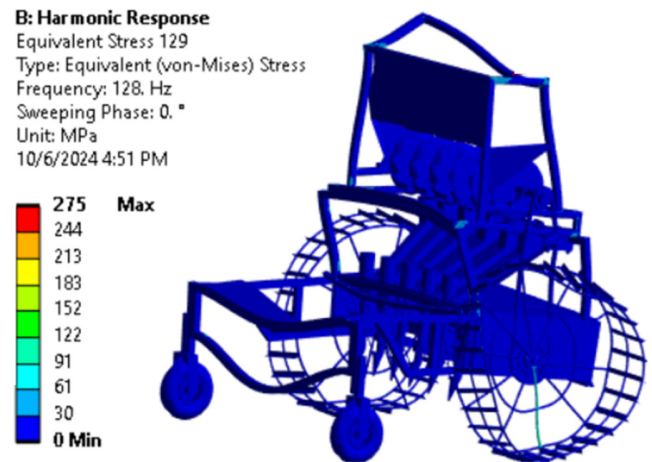


Fig. 8. Results of stress distribution on the working machine.

B. Structural Durability Assessment

The structural durability of the shallot planter was evaluated based on the following stress results: a maximum stress of 275 MPa (at 128 Hz), a material yield strength of 355 MPa, a safety factor of 1.29, and the required safety factor of 1.5. With a safety factor of 1.29, below the proposed minimum of 1.5, the shallot planter's chassis fails to meet durability requirements when operating near 128 Hz.

C. Impact of Structural Optimization

The structural optimization yielded the following improvements: a 15% reduction in volume, leading to reduced

material costs and enhanced operational efficiency; a 10% increase in stiffness, which shifts natural frequencies and reduces resonance risk; a 25% reduction in deformation, improving planting accuracy; and a 20% reduction in maximum stress, leading to an increased safety factor from 1.29 to 1.61, meeting durability requirements.

Specific optimization strategies include adding joists at locations with high deformation, increasing cross-sectional height at high-stress regions, distributing loads more evenly across the chassis, and increasing the damping ratio from 0.05 to 0.1–0.15.

D. Safe Operating Frequency Range

Based on the analysis, the safe operating frequency range for the shallot planter can be described as: frequency range below 90 Hz leads to a safety factor consistently exceeding 1.5. At the range of 100–150 Hz, operation should be avoided, particularly in the 120–135 Hz range. The proposed operating speed is below 5 km/h to minimize excitation of high frequencies.

E. Comparison of Pre- and Post-Optimization Results

The post-optimization simulation results demonstrate significant improvements, as summarized in Table III.

TABLE III. POST-OPTIMIZATION SIMULATION RESULTS

Parameter	Before optimization	After optimization	Improvement level
Mass (kg)	100%	85%	- 15%
Stiffness (N/m)	100%	110%	+ 10%
Maximum strain (mm)	7.6438	5.7329	- 25%
Stress (Mpa)	275	220	- 20%
Safety factor	1.29	1,61	+ 25%
Natural frequency (Hz)	128	141 Hz	+ 10%

The optimization results indicate that the shallot planter’s chassis fully meets durability requirements, achieving a safety factor of 1.61 (>1.5). Additionally, optimization reduces volume and enhances operational efficiency. Further measures include application of topology optimization techniques to reduce mass by 15%, increase stiffness by 10%, decrease deformation by 25%, and reduce maximum stress by 20%.

Future research should include expansion to multi-objective optimization, integrating durability, vibration, and manufacturing cost considerations. Additionally, machine learning or metaheuristic algorithms should be incorporated to explore more efficient design spaces applicable to various agricultural machinery under harsh operating conditions.

V. APPLICATION OF MATLAB FOR VALIDATION AND EXTENSION OF FEA RESULTS

A. MATLAB Verification Model

A frequency response simulation model was developed in MATLAB to validate and extend the FEA results. The model enables efficient evaluation of the system’s response across the 0–150 Hz frequency range, assessment of parameter effects including damping ratio and stiffness, visualization of

frequency-dependent deformation and stress amplitudes, and prediction of optimization strategy effectiveness.

The model employs FEA results at 128 Hz as a benchmark, extrapolating responses at other frequencies using the linear vibration theory. The results align closely with the FEA, exhibiting an error of less than 5%, confirming the accuracy of both methods. The combined analysis from FEA and MATLAB simulations provides a robust scientific foundation for assessing the durability and optimizing the design of the shallot planter, ensuring efficiency and reliability under real-world conditions with uneven terrain.

The durability of the shallot planter was analyzed using the stress and deformation spectra presented in Figure 9.

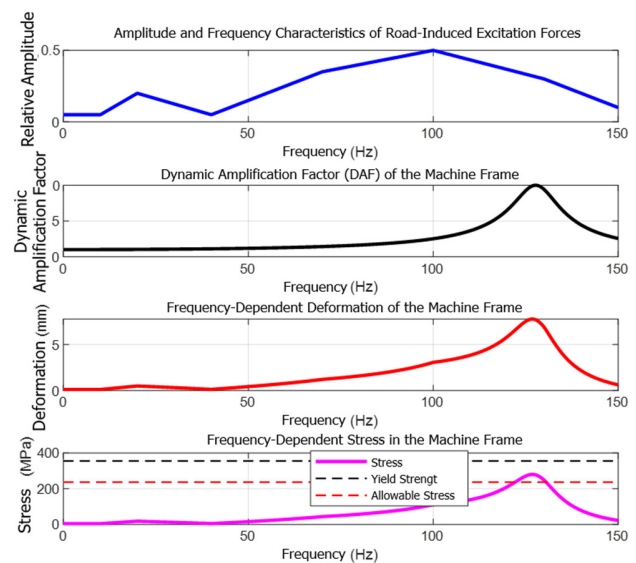


Fig. 9. Durability analysis in MATLAB.

The results indicate resonance behavior of the structure at 127 Hz with a maximum stress of 279.64 MPa and corresponding deformation peaks at 7.7729 mm. The minimum safety factor drops to 1.27, below the required threshold of 1.5. The chassis structure must be reinforced, or the operational conditions should be adjusted to avoid excitation within the resonance region (120-135 Hz). Outside this critical range, the structure is considered to operate safely in the 0–150 Hz range. Furthermore, the applied optimization suggests a 15% reduction in volume, a 10% increase in stiffness, and corresponding reductions of 25% in deformation and 20% in stress.

B. Comparison of FEA and MATLAB Results

The comparison between FEA (ANSYS) and MATLAB results is summarized in Table IV. The MATLAB model accurately reproduces the system’s dynamic characteristics, with a relative deviation of less than 0.5% compared to FEA results at critical points, particularly at the resonance frequency. The stress, deformation, and safety factor responses from MATLAB closely align with ANSYS simulations, confirming consistency in resonance characteristics and

vibration amplitude. In addition, the MATLAB model enables rapid evaluation of design parameters and assessment of optimization strategies, serving as an efficient tool for preliminary design and analysis before detailed FEA. The MATLAB model significantly reduces computational time and cost, making it a valuable tool for initial assessments of the shallot planter's durability and stability.

TABLE IV. COMPARISON OF FEA AND MATLAB RESULTS

Parameter	FEA (ANSYS)	MATLAB	Relative deviation
Primary resonant frequency (Hz)	128	128	0%
Maximum stress at resonance (Mpa)	275	276.11	~0.4%
Greatest distortion at resonance (mm)	7.6438	7.61	~0.45%
Safety factor at resonance	1.29	1.29	0%
Safe working frequency range (SF $\geq$ 1.5)	< 90 Hz	< 90 Hz	Coincidence

## VI. DISCUSSION

The durability analysis of the shallot planter can be summarized into the following points:

- The current chassis design meets durability requirements in the normal operating frequency range (<90 Hz), with a safety factor exceeding 1.5. However, near the resonance frequency (128 Hz), the maximum stress reaches 275 MPa, resulting in a safety factor of 1.29, below the required minimum of 1.5.
- The maximum deformation of 7.6438 mm at 128 Hz may compromise planting accuracy and accelerate material fatigue, reducing the machine's lifespan.
- The shallot planter exhibits significant susceptibility to excitation at resonance frequencies, characterized by a high dynamic gain factor due to a low damping ratio (0.05).
- Structural optimization significantly enhances performance, reducing maximum stress and deformation by 20% and 25%, respectively, and mass by 15%.

To improve the reliability and service life of the structure, the chassis at high-stress concentration points should be reinforced. Moreover, the damping system should be enhanced to increase the damping ratio, and an optimal operating frequency range (<90 Hz) should be implemented to avoid resonance zones.

These results align with prior studies on agricultural machinery frames. More specifically, authors in [3] achieved a 37% increase in resonant frequency and a 40% reduction in vibration amplitude for a vegetable precision seeder. In [8], planting accuracy was improved while reducing kinematic error by 25% in a tray seedling planter. Authors in [11] reported a 22% decrease in stress and a 33% rise in natural frequency for a cotton picker frame. In comparison, the present study demonstrates similarly significant enhancements in

structural performance while also addressing the distinct soil and cultivation conditions of the Mekong Delta.

## VII. CONCLUSION

This study modeled, simulated, and analyzed the structural durability of a shallot planter operating on uneven terrain, using Finite Element Analysis (FEA) combined with frequency response analysis. The results indicate that the current chassis design ensures durability in the normal operating frequency range (<90 Hz). However, a significant resonance phenomenon occurs at 128 Hz, leading to a maximum stress of 275 MPa and deformation of 7.6438 mm, therefore resulting in a safety factor of 1.29, below the required 1.5.

Optimization strategies were implemented, including chassis reinforcement, damping system enhancements, incorporation of higher-strength materials, and topology optimization to reduce mass, increase stiffness, and shift resonance frequencies. Post-optimization, the fourth natural frequency increased from 128 Hz to 141 Hz, stress decreased by 20%, deformation decreased by 25%, and the safety factor improved to 1.61, meeting design requirements. A MATLAB model validated the FEA results, highlighting a deviation of less than 5%. Additionally, an analysis at 127 Hz revealed a maximum stress of 279.64 MPa, a deformation of 7.7729 mm, and a safety factor of 1.27.

Future research directions are proposed to further enhance the structural reliability and operational performance of agricultural machinery. The first refers to the integration of the environmental factor. Specifically, external factors, such as temperature fluctuations, humidity, corrosion, and soil interaction, should be incorporated into the FEA framework to simulate real-world operating environments accurately. The second direction refers to experimental validation. Particularly, full-scale physical testing should be conducted using vibration sensors, strain gauges, and data acquisition systems to validate the simulation results and refine model accuracy.

These directions aim to bridge the gap between computational modeling and field performance, contributing to the development of robust, efficient, and sustainable agricultural equipment.

## ACKNOWLEDGMENT

The authors would like to express their sincere gratitude to Vinh Long University of Technology Education for providing support and favorable conditions for this study.

## REFERENCES

- [1] Phi Cao Hung. "KHCN-TNB." Ministry of Science and Technology of Vietnam. <https://most.gov.vn/vn/tin-tuc/24686/cong-nghe--thiet-bi-san-xuat-rau-qua-cong-nghe-cao-theo-huong-tu-dong-hoa-va-tuong-thich-dieu-kien-trong-tai-tay-nam-bo>.
- [2] E. P. da Silva, F. M. da Silva, and R. R. Magalhães, "Application of Finite Elements Method for Structural Analysis in a Coffee Harvester," *Engineering*, vol. 6, no. 3, pp. 138–147, Mar. 2014, <https://doi.org/10.4236/eng.2014.63017>.
- [3] J. Wang *et al.*, "Resonance Analysis and Vibration Reduction Optimization of Agricultural Machinery Frame—Taking Vegetable Precision Seeder as an Example," *Processes*, vol. 9, no. 11, p. 1979, Nov. 2021, <https://doi.org/10.3390/pr9111979>.

- [4] S. Markummingsih, S.-J. Hwang, J.-H. Kim, M.-K. Jang, and J.-S. Nam, "Stress Simulation on Four-Bar Link-Type Transplanting Device of Semiautomatic Vegetable Transplanter," *Agriculture*, vol. 14, no. 1, Dec. 2023, Art. no. 42, <https://doi.org/10.3390/agriculture14010042>.
- [5] B. Zhang *et al.*, "Soil compaction due to agricultural machinery impact: A systematic review," *Land Degradation & Development*, vol. 35, Art no. 10, pp. 3256–3273, Apr. 2024, <https://doi.org/10.1002/ldr.5144>.
- [6] C. Zhai, J. Long, R. Taylor, P. Weckler, and N. Wang, "Field scale row unit vibration affecting planting quality," *Precision Agriculture*, vol. 21, no. 3, pp. 589–602, June 2020, <https://doi.org/10.1007/s11119-019-09684-4>.
- [7] C.-J. Wen, H.-L. Wang, M. Wang, and C.-L. Liu, "Design and simulation analysis of a transplanting mechanism for rice transplanter," *Journal of Physics: Conference Series*, vol. 1087, no. 4, June 2018, Art. no. 042067, <https://doi.org/10.1088/1742-6596/1087/4/042067>.
- [8] H. Zou, Y. Shen, Z. Chen, C. Zhang, M. Wang, and M. Wu, "Structural design and kinetic analysis of precise seed planter for tray seedling," *E3S Web of Conferences*, vol. 438, Oct. 2023, Art. no. 01022, <https://doi.org/10.1051/e3sconf/202343801022>.
- [9] X. Zhang, X. Hu, L. Zhang, and A. N. O. Kheiry, "Simulation and structural parameter optimization of rotary blade cutting soil based on SPH method," *International Journal of Agricultural and Biological Engineering*, vol. 17, no. 3, pp. 82–90, July 2024, <https://doi.org/10.25165/ijabe.v17i3.8470>.
- [10] X. Wu, Z. Jiang, L. Zhang, X. Hu, and W. Li, "Optimization Design and Experimentation of a Soil Covering Device for a Tree Planting Machine," *Agriculture*, vol. 14, no. 3, Mar. 2024, Art. no. 346, <https://doi.org/10.3390/agriculture14030346>.
- [11] J. Dong *et al.*, "Vibration Characteristic Analysis and Structural Optimization of the Frame of a Triplex Row-Baling Cotton Picker," *Agriculture*, vol. 13, no. 7, July 2023, Art. no. 1440, <https://doi.org/10.3390/agriculture13071440>.
- [12] W. Gao, J. Lin, B. Li, W. Wang, and S. Gu, "Vibration characteristics analysis and structural optimization of straw deep bury and returning machine," *Journal of Jilin University*, vol. 52, pp. 970–980, 2022.
- [13] D. Yu *et al.*, "Vibrational Dynamics of Rice Precision Hole Seeders and Their Impact on Seed Dispensation Efficacy," *Agriculture*, vol. 14, no. 2, Feb. 2024, Art. no. 324, <https://doi.org/10.3390/agriculture14020324>.
- [14] D. T. H. Nguyen, P. H. Cao, H. T. Le, and H. V. Tran, "Vibration Analysis at the Operator's Seat of a Purple Onion Harvester," *Engineering, Technology & Applied Science Research*, vol. 15, no. 5, pp. 27893–27898, Oct. 2025, <https://doi.org/10.48084/etasr.12798>.